Contrast Enhancement in Digital Imaging using Histogram Equalization

David Menotti
Universidade Federal de Ouro Preto
Departamento de Computação
35.400-000, Ouro Preto-MG, Brazil
menottid@gmail.com

Arnaldo de A. Araújo and Gisele L. Pappa
Universidade Federal de Minas Gerais
Departamento de Ciência da Computação
31.270-010, Belo Horizonte-MG, Brazil
{arnaldo,glpappa}@dcc.ufmg.br

Laurent Najman
Université Paris-Est
UMR CNRS 8049 - A2SI-ESIEE
93162, Noisy-le-Grand, France
l.najman@esiee.fr

Jacques Facon
Pontifícia Universidade Católica do Paraná
Departamento de Informática
80.215-901, Curitiba-PR, Brazil
facon@ppgia.pucpr.br

Abstract

This work proposes two methodologies for fast image contrast enhancement based on histogram equalization (HE), one for gray-level images, and other for color images. For gray-level images, we propose a technique called Multi-HE, which decomposes the input image into several sub-images, and then applies the classical HE process to each one of them. In order to decompose the input image, we propose two different discrepancy functions, conceiving two new methods. Experimental results show that both methods are better in preserving the brightness and producing more natural looking images than other HE methods. For color images, we introduce a generic fast hue-preserving histogram equalization method based on the RGB *color space, and two instantiations of the proposed generic method, using $1D$ and $2D$ histograms. HE is performed using shift hue-preserving transformations, avoiding the appearance of unrealistic colors. Experimental results show that the value of the image contrast produced by our methods is in average 50% greater than the value of contrast in the original image, still keeping the quality of the output images close to the original.*

1. Introduction

Nowadays digital cameras are certainly the most used devices to capture images. They are everywhere, including mobile phones, personal digital assistants (PDAs - a.k.a. pocket computers or palmtop computers), robots, and surveillance and home security systems. There is no doubt that the quality of the images obtained by digital cameras, regardless of the context in which they are used, has improved a lot since digital cameras early days. Part of these improvements are due to the higher processing capability of the systems they are built-in and memory availability. However, there are still a variety of problems which need to be tackled regarding the quality of the images obtained, including: 1) contrast defects; 2) chromatic aberrations; 3) various sources of noises; 4) vignetting; 5) geometrical distortions; 6) color demosaicing; and 7) focus defects.

Among the seven problems related above, some are more dependent on the quality of the capture devices used (like 2-7), whereas others are related to the conditions in which the image was captured (such as 1). When working on the latter, the time required to correct the problem on contrast is a big issue. This is because the methods developed to correct these problems can be applied to an image on a mobile phone with very low processing capability, or on a powerful computer.

Moreover, in real-time applications, the efficiency of such methods is usually favored over the quality of the images obtained. A fast method generating images with medium enhancement on image contrast is worth more than a slow method with outstanding enhancement.

With this in mind, this work[1] proposes two methodologies for contrast enhancement in digital imaging using histogram equalization (HE)[2]. Although there has been a lot of

1 This paper comes from the doctoral thesis of David Menotti [10], submitted to the Department of Computer Science, Universidade Federal de Minas Gerais, in April 2008.

2 In this work, the contrast is defined as the standard variation of the image gray-levels or luminance.

research in the image enhancement area for 40 years [5, 10], there is still a lot of room for improvement concerning the quality of the enhanced image obtained and the time necessary to obtain it.

HE is a histogram specification process [3] which consists of generating an output image with a uniform histogram (*i.e.*, uniform distribution). In image processing, the idea of equalizing a histogram is to stretch and/or redistribute the original histogram using the entire range of discrete levels of the image, in a way that an enhancement of image contrast is achieved. HE is a technique commonly used for image contrast enhancement, since it is computationally fast and simple to implement. Our main motivation is to preserve the best features the HE methods have, and introduce some modifications which will overcome the drawbacks associated with them.

In the case of **gray-level image contrast enhancement**, methods based on HE have been the most used. Despite its success for image contrast enhancement, this technique has a well-known drawback: it does not preserve the brightness[3] of the input image on the output one. This problem makes the use of classical HE techniques [5] not suitable for image contrast enhancement on consumer electronic products, such as video surveillance, where preserving the input brightness is essential to avoid the generation of non-existing artifacts in the output image [14, 10].

In order to overcome this problem, variations of the classic HE technique, such as [6, 22, 2, 1], have proposed to first decompose the input image into two sub-images, and then perform HE independently in each sub-image (Bi-HE). These works mathematically show that dividing the image into two rises the expectance of preserving the brightness. Although Bi-HE successfully performs image contrast enhancement and also preserves the input brightness to some extend, it might generate images which do not look as natural as the input ones. Unnatural images are unacceptable for use in consumer electronics products [14, 10].

Hence, in order to enhance contrast, preserve brightness and produce natural looking images, we propose a generic Multi-HE (MHE) method that first decomposes the input image into several sub-images, and then applies the classical HE process to each of them. We present two discrepancy functions to decompose the image, conceiving two variants of that generic MHE method for image contrast enhancement, *i.e.*, Minimum Within-Class Variance MHE (MWCVMHE) and Minimum Middle Level Squared Error MHE (MMLSEMHE). Moreover, a cost function, which takes into account both the discrepancy between the input and enhanced images and the number of decomposed sub-images, is used to automatically determine in how many sub-images the input image will be decomposed on.

Regarding **color image contrast enhancement**, the classical methods are also based on HE. The extension of HE methods to color images is not straightforward, because there are some particular properties of color images that need to be properly taken into account during image contrast enhancement. These properties include the luminance (*L*) (or intensity (*I*)), saturation (*S*), and hue (*H*) attributes of the color.

The luminance represents the achromatic part of the color (*e.g.*, it can be defined as a weighted function of the R (red), G (green), and B (blue) color channels), whereas the saturation and hue refer to the chromatic part of the image. The saturation can be seen as measure of how much white is present in the color, and the hue is the attribute of the color which decides its "real color", *e.g.*, red or green. For the purpose of enhancing a color image, the hue should not be changed for any pixel, avoiding output images with unnatural aspect.

Color spaces such as *HSV*, *HSI*, *CIELUV*, and *CIELAB* were conceived based on these three attributes. However, color images in digital devices, such as mobile phones, cameras, and PDAs, are commonly transmitted, displayed, and stored in the *RGB* color space (*i.e.*, R-red, G-green, and B-blue). This color space is not the most appropriated one for image processing tasks, since the meaning of the attribute colors is not explicitly separated as it would be in other color spaces. The conversion from the *RGB* color space to a Luminance-Hue-Saturation (*LHS*)-based color space is trivial, but can be both not suitable for real-time applications and the digital devices referred above. Moreover, working on a *LHS*-based color space requires tackling the well-known gamut problem [16].

The literature of HE methods for color image contrast enhancement presents works based on the *RGB*, *LHS*, *CIELUV*, and other color spaces. Neither methods based on the *RGB* color space nor methods based on other color spaces present all the characteristics required for use in portable devices: to be fast, improve the images contrast and still preserve the hue. Methods based on the *RGB* space do not preserve the hue, while methods based on other color spaces are slower due to conversions required among color spaces and may also be not hue-preserving. In order to achieve all these three requirements, this work presents a generic fast hue-preserving HE method based on the *RGB* color space for image contrast enhancement.

From the generic method we create two variants, which are characterized by the histograms dimension they use, *i.e.*, $1D$ or $2D$. The equalization is performed by hue-preserving transformations directly in the *RGB* color space, avoiding the gamut problem, keeping the hue unchanged, and the requirement of conversion between color spaces. Moreover,

3 In this work, the brightness is defined as the mean of the image gray-levels

our methods improve the image contrast (*i.e.*, improve the variance on the luminance attribute) and, simultaneously, the saturation is modified according to the equalization of the RGB histogram. The methods estimate the *RGB* $3D$ histogram to be equalized through R, G, and B $1D$ histograms and RG, RB, and GB $2D$ histograms, respectively, yielding algorithms with time and space complexities linear with respect to the image dimension. These characteristics make these methods suitable for real-time applications.

The remainder of this work is organized as follows. Section 2 present the Multi-HE methods for gray-level images, whilst Section 3 introduces our fast hue-preserving HE for color images. Section 4 shows some experimental results, and finally conclusions are pointed out in Section 5.

2. Multi-Histogram Equalization Methods for Contrast Enhancement and Brightness Preserving

As mentioned before, the classic HE method enhances the contrast of an image but cannot preserve its brightness (which is shifted to the middle gray-level value). As a result, it can generate unnatural and non-existing objects in the processed image. In contrast, Bi-HE methods [6, 22, 2, 1] can produce a significant image contrast enhancement and, to some extend, preserve the brightness of the image. However, the generated images might not have a natural appearance [14, Figure 1]. To surmount such drawbacks, the main idea of our proposed methods is to decompose the image into several sub-images, such that the image contrast enhancement provided by the HE in each sub-image is less intense, leading the output image to have a more natural look. The conception of this method arises two questions.

The first question is how to decompose the input image. As HE is the focus of the work, the image decomposition process is based on the histogram of the image. The histogram is divided into classes determined by threshold levels, where each histogram class represents a sub-image. The decomposition process can be seen as an image segmentation process executed through multi-thresholding selection [7]. The second question is in how many sub-images an image should be be decomposed on. This number is directly related to how the input image is decomposed.

In order to answer these questions, Section 2.1 presents two functions to decompose an image based on threshold levels, whereas the algorithm used to find the optimal threshold levels is presented in Section 2.2. Finally, a criterion for automatically select the number of decomposed sub-images is exposed in Section 2.3.

Note that the methods described in this section are published in [14].

2.1. Multi-Histogram Decomposition

Many HE-based methods have been proposed in the literature to decompose an image into sub-images by using the value of some statistical measure based on the image gray-level [6, 22, 2, 1]. These methods aim to optimize the entropy or preserve the brightness of the image. Here, we will focus our attention on decomposing an image such that the enhanced images still have a natural appearance. For such aim, we propose to cluster the histogram of the image into classes, where each class corresponds to a sub-image. By doing that, we want to minimize the brightness shift yielded by HE process into each sub-image. By minimizing this shift, we expect to preserve both the brightness and the natural appearance of the processed image.

From the multi-threshold selection literature point of view, the problem stated above can be seen as the minimization of the within-histogram class variance (the well-know Otsu method [18]), where the within-class variance is the total squared error of each histogram class with respect to its mean value (*i.e.*, the brightness). That is, the decomposition aim is to find the optimal threshold set $T^k = \{t_1^k, ..., t_{k-1}^k\}$ that minimizes the decomposition error of the histogram of the image into k histogram classes, and decomposes the image $I[0, L-1]$ into k sub-images $I[l_s^{1,k}, l_f^{1,k}], ..., I[l_s^{k,k}, l_f^{k,k}]$. $l_s^{j,k}$ and $l_f^{j,k}$ are the lower and upper gray-level boundaries of each sub-image j when the image is decomposed into k sub-images, and are defined as: $l_s^{j,k} = t_{j-1}^k$, if $j > 1$, and $l_s^{j,k} = 0$ otherwise, and $l_f^{j,k} = t_j^k + 1$, if $j \neq k$, and $l_f^{j,k} = L-1$ otherwise. The discrepancy function for decomposing the original image into k sub-images following the minimization of within-class variance can be expressed as

$$Disc(k) = \sum_{j=1}^{k} \sum_{l=l_s^{j,k}}^{l_f^{j,k}} (l - l_m(I[l_s^{j,k}, l_f^{j,k}]))^2 P_l^{I[0,L-1]}. \tag{1}$$

The method conceived with this discrepancy function will be called Minimum Within-Class Variance MHE method (MWCVMHE). Note that the mean gray-level (*i.e.*, the brightness) of each sub-image processed by the CHE method is theoretically shifted to the middle gray-level of its range, *i.e.*, $l_m(O[l_s, l_f]) = l_{mm}(I[l_s, l_f]) = l_{mm}(O[l_s, l_f]) = (l_s + l_f)/2$. As we want to minimize the brightness shift of each processed sub-image such that the global processed image has its contrast enhanced and its brightness preserved (creating a natural looking output image), we focus our attention on the brightness of the output image. Hence, instead of using the mean $l_m(I[l_s, l_f])$ of each sub-image $I[l_s, l_f]$ in the discrepancy function, we propose to use its middle level $(l_s + l_f)/2$, since every enhanced sub-image

$O[l_s, l_f]$ will theoretically have its mean value (brightness) on the middle level of the image range - thanks to the specification of a uniform histogram distribution. Therefore, a new discrepancy function is proposed and it is expressed as

$$Disc(k) = \sum_{j=1}^{k} \sum_{l=l_s^{j,k}}^{l_f^{j,k}} (l - l_{mm}(I[l_s^{j,k}, l_f^{j,k}]))^2 P_l^{I[0,L-1]}, \tag{2}$$

where $l_{mm}(I[l_s^{j,k}, l_f^{j,k}])$ stands for the middle value of the image $I[l_s^{j,k}, l_f^{j,k}]$ and it is defined as $||(l_s + l_f)/2||$. The method conceived with this discrepancy function will be called Minimum Middle Level Squared Error MHE method (MMLSEMHE).

2.2. Finding the Optimal Thresholds

The task of finding the optimal $k-1$ threshold leves which segment an image into k classes can be easily performed by a dynamic programming algorithm with $O(kL^2)$ time complexity [7]. Algorithm 1 shows the pseudocode of this algorithm, where $\varphi(p,q)$ stands for the "discrepancy contribution" of the sub-image $I[p,q]$, *i.e.*,

$$\varphi(p,q) = \sum_{l=p}^{q} (l-\gamma)^2 P_l^{I[0,L-1]}, \tag{3}$$

where γ stands for $l_m(I[p,q])$ or $l_{mm}(I[p,q])$, depending on the discrepancy function used (see Equations 1 and 2).

Once Algorithm 1 is run, the optimal threshold vector T^k can be obtained through a back-searching procedure on PT, *i.e.*,

$$t_j^k = PT(j+1, t_{j+1}^{k*}), \tag{4}$$

where $1 \leq j < k$, $t_{j+1}^{k*} = L-1$ if $j+1 = k$, and $t_{j+1}^{k*} = t_{j+1}^{k}$ otherwise.

2.3. Automatic Thresholding Criterium

This section presents an approach to automatically choose in how many sub-images the original image should be decomposed on. This decision is a key point of our work, which has three main aims: 1) contrast enhancement; 2) brightness preserving; 3) natural appearance. Nonetheless, these goals cannot be all maximize simultaneously. We take into account that as the number of sub-images in which the original image is decomposed increases, the chance of preserving the image brightness and natural appearance also increases. However, the chances of enhancing the image contrast decrease. To decide in how many sub-images the original image should be decomposed on, a tradeoff between brightness, natural appearance and contrast should be considered. Hence, we propose to use a cost function, initially used in [23], to automatically select the number of decomposed sub-images. This cost function takes into account both the discrepancy between the original and processed images (which is our own aim decomposition function) and the number of sub-images to which the original image is decomposed, and it is given as

$$C(k) = \rho(Disc(k))^{1/2} + (\log_2(k))^2, \tag{5}$$

where ρ is a positive weighting constant. The number of decomposed sub-images k is automatically given as the one which minimizes the cost function $C(k)$. It is shown in [23] that the cost function presented in Equation 5 has a unique minimum. Hence, instead of finding the value k which minimizes $C(k)$ throughout k values range, it is enough to search for k from 0 up to the point $C(k)$ starts to increase.

Algorithm 1: Computing $Disc(k)$ and $PT(k, L-1)$

Data: $\varphi(p,q)$ - discrepancy of sub-image $I[p,q]$
Result: $D(p)_q$ - discrepancy function $Disc(p)$ up to level q
Result: PT - optimum thresholds matrix

for $q \leftarrow 0$; $q < L$; $q{+}{+}$ **do** $D(1)_q \leftarrow \varphi(0,q)$;
for $p \leftarrow 1$; $p \leq k$; $p{+}{+}$ **do**
  $D(p+1)_p \leftarrow D(p)_{p-1} + \varphi(p-1, p-1)$;
  $PT(p+1, p) \leftarrow p-1$;
  for $q \leftarrow p+1$; $q \leq L-k+p$; $q{+}{+}$ **do**
    $D(p+1)_q \leftarrow -\infty$;
    for $l \leftarrow p-1$; $l \leq q-1$; $l{+}{+}$ **do**
      if $(D(p+1)_q > D(p)_l + \varphi(l+1, q))$ **then**
        $D(p+1)_q \leftarrow D(p)_l + \varphi(l+1,q)$;
        $PT(p+1, q) \leftarrow l$;

3. Fast Hue-Preserving Histogram Equalization Methods for Color Image Contrast Enhancement

This section presents a generic method that, in contrast with the classical method presented in [5] (frow now on C1DHE method) and the one in [20] (from now on TV3DHE method), is both hue-preserving and has time and space complexities which complies with real-world and real-time applications. We propose two variants of this generic method, which are characterized by the histogram dimensions used to estimate the $3D$ probability functions, *i.e.*, $1D$ or $2D$ histograms.

3.1. Generic Hue-preserving Histogram Equalization Method

Our generic hue-preserving HE method is divided in three phases. Let I and O be the input and output images, respectively. Let the input $\#D$ histograms and probability functions be defined as in [15, Section 2] and [10, Section 4.1] (omitted due to space constraints), where $\#$ is the histogram dimension used (the variant point of our method). The first phase of our method consists of computing the $\#D$ histograms of I. Although the proposed method works with $\#D$ histograms and probability functions, we do not equalize the $\#D$ histograms per say, but a $3D$ pseudo-histogram, $H'^{I^{RGB}}$. Indeed, the equalization of $H'^{I^{RGB}}$ is based on a pseudo $3D$ cumulative density function, built through probability density functions.

The computation of this cumulative density function, $C'^{I^{RGB}}$, which constitutes the second phase of our method, is performed as the product of the three $\#D$ cumulative functions. We show in details the variant methods in Sections 3.2 and 3.3.

The third phase works as follows. Let $H^{O^{RGB}}$ be the uniform histogram of the output image, where any entry (R_o, G_o, B_o) has the same amount of pixels, since such output histogram is desired, *i.e.*,

$$H^{O^{RGB}}_{R_o,G_o,B_o} = \frac{1}{L^3}(mn), \tag{6}$$

or any entry (R_o, G_o, B_o) in $P^{O^{RGB}}$ has the same density, *i.e.*,

$$P^{O^{RGB}}_{R_o,G_o,B_o} = 1/L^3. \tag{7}$$

Hence, any entry (R_o, G_o, B_o) in $C^{O^{RGB}}$ is directly computed using $P^{O^{RGB}}$, *i.e.*,

$$C^{O^{RGB}}_{R_o,G_o,B_o} = (R_o+1)(G_o+1)(B_o+1)/L^3. \tag{8}$$

To yield the output enhanced image, for every input pixel $(x, y) \in X$, where $(R_i, G_i, B_i) = I^{RGB}(x, y)$, we obtain the smallest $(R_o, G_o, B_o) = O^{RGB}(x, y)$ for which the inequality

$$|C'^{I^{RGB}}_{R_i,G_i,B_i} - C^{O^{RGB}}_{R_o,G_o,B_o}| \geq 0, \tag{9}$$

holds.

However, this step of calculating the output pixel value presents an ambiguity, mainly because there are many possible solutions for (R_o, G_o, B_o) which satisfy Equation 9. This ambiguity is remedied as follows. Unlike the method described in [20] (TV3DHE method), which iteratively increased or decreased the values of R_o, G_o, and B_o in order to minimize Equation 9, we propose to find the output triplet (R_o, G_o, B_o) for any image pixel in a single step, *i.e.*, $O(1)$. Thus, from Equations 8 and 9, we have

$$C'^{I^{RGB}}_{R_i,G_i,B_i} - \frac{(R_o+1)(G_o+1)(B_o+1)}{L^3} = 0. \tag{10}$$

If we take R_o, G_o, and B_o as $R_i + k$, $G_i + k$, and $B_i + k$, respectively, where k is the number of iterations required for minimizing Equation 9, we obtain

$$\begin{aligned} &k^3+ \\ &k^2[R_i^{'} + G_i^{'} + B_i^{'}]+ \\ &k[R_i^{'} \times G_i^{'} + R_i^{'} \times B_i^{'} + G_i^{'} \times B_i^{'}]+ \\ &R_i^{'} \times G_i^{'} \times B_i^{'} - L^3 \times C'^{I^{RGB}}_{R_i,G_i,B_i} = 0. \end{aligned} \tag{11}$$

where $R_i^{'}$, $G_i^{'}$, and $B_i^{'}$ mean $R_i + 1$, $G_i + 1$, and $B_i + 1$, respectively. By solving this cubic equation in function of k, we obtain the desired output triplet (R_o, G_o, B_o) as the input one plus the displacement k, *i.e.*, $(R_i + \langle k \rangle, G_i + \langle k \rangle, B_i + \langle k \rangle)$, where $\langle k \rangle$ stands for the nearest integer to $k \in \mathbb{R}$.

Equation 11 can be easily solved by [17] or by the classical Cardan's methods which use transcendental functions. As the former method is faster and mathematically simpler than the latter, we chose to use it.

Observe that any image pixel is enhanced following a shift transformation by a k factor, *i.e.*, from (R_i, G_i, B_i) to $(R_o, G_o, B_o) = (R_i + k, G_i + k, B_i + k)$, which makes our generic method hue-preserving [16].

Having described this generic method, the next subsections show our variant methods, which differ only on the histogram dimension used. By respecting the chronology's conception of our methods, the method based on RG, RB, and GB $2D$ histograms [12] (from now on HP2DHE method), is described first in Section 3.2. Then, the method based on $1D$ histograms [13] (from now on HP1DHE method) is presented in Section 3.3.

3.2. Hue-preserving 2D Histogram Equalization

In this section, we present our HP2DHE method, initially introduced in [12]. It uses $2D$ histograms (as defined in [15, Section 2] and [10, Section 4.1]) and is based on the joint probability distribution functions of channels two-at-a-time to perform HE. The cumulative probability density function (or the probability distribution function), $C'^{I^{RGB}}$, is computed as the product of the three $2D$ cumulative functions for any entry (R_i, G_i, B_i), *i.e.*,

$$C'^{I^{RGB}}_{R_i,G_i,B_i} = C^{I^{RG}}_{R_i,G_i} C^{I^{RB}}_{R_i,B_i} C^{I^{GB}}_{G_i,B_i}. \tag{12}$$

For details on how to directly calculate $C^{I^{RG}}$, $C^{I^{RB}}$, and $C^{I^{GB}}$ through the probability density function $P^{I^{RG}}$, $P^{I^{RB}}$, and $P^{I^{GB}}$ see [15, Section 2] or [10, Section 4.1]. The main rationale for computing this pseudo-cumulative density function as the product of three $2D$ cumulative density functions is that the three channels in an image are usually not simultaneously correlated.

Image	HE	BBHE	DSIHE	MMBEBHE	BPHEME	RMSHE	MWCVMHE	MMLSEMHE
arctichare	8.11	16.63	13.09	23.55	22.95	30.74	31.44	40.27
bottle	12.88	18.68	17.53	28.44	25.72	29.68	35.99	36.71
copter	10.61	15.95	14.20	25.50	23.20	25.62	33.83	34.77
couple	7.57	13.18	11.61	19.86	38.54	19.65	30.59	40.16
Einstein	15.08	15.15	15.58	18.91	16.21	19.51	31.42	34.53
F16	11.92	20.69	16.02	20.32	21.61	22.72	24.43	37.10
girl	13.03	13.30	12.99	14.03	13.19	28.00	29.39	33.03
hands	4.36	19.58	17.76	19.99	17.18	30.93	24.49	35.82
house	10.82	14.27	14.07	21.41	19.93	21.36	31.81	36.37
jet	9.51	22.50	14.37	30.78	23.99	27.85	29.14	31.74
U2	6.99	15.06	10.94	19.87	27.32	22.12	26.21	31.08
woman	17.83	17.73	18.25	21.60	19.23	23.67	28.83	34.53

Table 1. $PSNR = 10 \times \log_{10}(L-1)^2/MSE$

Note that, in [13], we proposed to solve Equation 9 iteratively, as done in [20], by using a non hue-preserving transformation. Here, we modify the method originally proposed in [13] to use the hue-preserving shift transformation and the solution of Equation 9 described in the previous subsection. These two modifications make the HP2DHE method presented here hue-preserving, and reduces its time complexity from $O(max(mnL, L^2))$ to $O(max(mn, L^2))$.

3.3. Hue-preserving 1D Histogram Equalization

In this section, we present a hue-preserving HE method based on the RGB color space for image contrast enhancement, which uses $1D$ histograms, and is also a variant of the generic method described in Section 3.1. The method is based on the independence assumption of color channels, which is used for computing the cumulative density function.

We use $1D$ histograms to estimate a $3D$ probability distribution function (or a cumulative density function), and then equalize the conceived histogram through the estimated function. Hence, the function $C^{I^{RGB}}$ is estimated for any entry (R_i, G_i, B_i) as the product of every probability distribution function $C^{I^R}_{R_i}$, $C^{I^G}_{G_i}$, and $C^{I^B}_{B_i}$, following the rule, *i.e.*,

$$C'^{I^{RGB}}_{R_i,G_i,B_i} = C^{I^R}_{R_i} C^{I^G}_{G_i} C^{I^B}_{B_i}. \qquad (13)$$

For details on how to directly calculate C^{I^R}, C^{I^G}, and C^{I^B} through P^{I^R}, P^{I^G}, and P^{I^B} see [15, Section 2] or [10, Section 4.1]. Note that, in Equation 13, $C'^{I^{RGB}}$ is defined with a correct dimensional meaning, *i.e.*, $C'^{I^{RGB}}$, a $3D$ cumulative function, is computed as the product of three $1D$ cumulative functions, while in Equation 12 $C'^{I^{RGB}}$ is defined with a wrong dimensional meaning, *i.e.*, $C'^{I^{RGB}}$ is computed as the product of three $2D$ cumulative functions. Nevertheless, the images processed by the HP2DHE method produce similar results to the HP1DHE method, as the experiments reported in Section 4.

As we use $1D$ histograms, this method has a smaller time complexity than the HP2DHE method, *i.e.*, $O(max(mn, L))$, and the space complexity is linear, *i.e.*, $O(L)$. Moreover, the time and space complexities of HP1DHE are exactly the same of the C1DHE method, which are the best to our knowledge.

A complete description of the methods presented in this section can be found in [15, 10].

4. Experiments

In this section, we report experiments performed to compare and evaluate the methods proposed in Sections 2 and 3. Section 4.1 presents the experiments involving methods proposed for handling gray-level images, and Section 4.2 analyzes and discusses the experimental results concerning the methods proposed for handling color images.

4.1. Experiments with Gray-level Images

In this section, we report results of experiments comparing our proposed methods with other HE methods (HE, BBHE, DSIHE, MMBEBHE, and RMSHE ($r = 2$)) and the method proposed in [21]. The input images used in the experiments were the ones previously used in [6, 22, 2, 1, 21]. They are named as they were in the works where they first appeared: arctic hare, bottle, copter, couple, Einstein, F16, girl, hands, house, jet, U2, woman (girl in [21]). Images were extracted from the CVG-UGR database [4] and provided by the authors of [2, 1].

Besides an analyzes of brightness (the mean) and contrast (the standard deviation) values of the original and out-

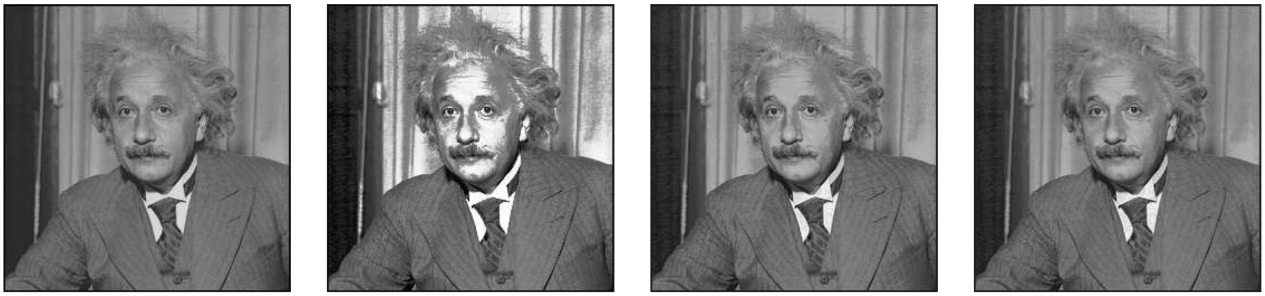

Figure 1. From left to right: the Einstein original, enhanced RMSHE $(r = 2)$, MWCVMHE $(k = 6)$, and MMLSEMHE $(k = 7)$ images.

put images, in order to assess the appropriateness of the processed images for consumer electronics products, for each image, we compute the $PSNR$ measure [19]. In image processing literature, the $PSNR$ has been used as a standard measure to evaluate and compare compression and segmentation algorithms [19]. It is well-known that a processed image with good quality (with respect to the original one) presents $PSNR$ values within 30 db and 40 db [19].

Due to space constraints, the analysis of brightness and contrast of the original and the output images obtained by the HE methods was omitted and it is presented in [14, 10]. The values of $PSNR$ obtained for each image are presented in Table 1. This table is divided into three parts: 1) The names of original images; 2) The data values obtained by the Uni- and Bi-HE methods, *i.e.*, HE, BBHE, DSIHE, MMBEBHE, and BPHEME; 3) The values obtained by the MHE methods, *i.e.*, RMSHE ($r = 2$), and our proposed MWCVMHE and MMLSEMHE.

For each image in Table 1, we highlight the best data values in the second and third parts of the table in either dark or light gray. We then compare these best values in the second and third parts of the table against each other (*i.e.*, Uni- and Bi-HE methods against MHE methods). The best value is dark-grayed, the worst light-grayed. Recall that the greater the value of the $PSNR$, the better it is.

Analyzing the data presented in Table 1, we observe that the images processed by the MMLSEMHE method produces the best $PSNR$ values, as they are within the range $[30 \text{ db}, 40 \text{ db}]$. Hence, we can argue that the MMLSEMHE method performs image contrast enhancement and brightness preserving while still producing images with a natural looking. Moreover, this result corroborates, in practice, our hypothesis that the MMLSEMHE method, using the discrepancy function in Equation 2, yields images with the best $PSNR$ values among all HE methods.

Besides this $PSNR$ analysis, we also perform an image visual assessment. Remark that all the 12 input images, their histograms, their respective enhanced images and equalized histograms (obtained by all the method listed in Table 1), adding up more than 200 images, can be seen in [9]. Here, we show the images obtained by the image Einstein.

Figure 1 shows the Einstein image and the resulting images obtained by the MHE methods, *i.e.*, RMSHE (with $r = 2$), MWCVMHE, and MMLSEMHE. By observing the processed images, it is noticeable that our proposed methods are the only ones among the MHE methods that can produce natural looking images.

After analyzing the data presented in Table 1 and visually observing the processed images, we can conclude that the MMLSEMHE method produces images with better quality than the other methods with respect to the $PSNR$ measure. By further analyses made in [14, 10], we can also conclude that: 1) A better image contrast enhancement can be obtained by the MWCVMHE method, which also presents satisfactory brightness preserving and natural looking images; 2) The RMSHE method ($r = 2$) should be employed if even more contrast enhancement than offered by the the MMLSEMHE and MWCVMHE methods is desired. However, in this case, the processed image may present some annoying and unnatural artifacts (for instance Figure 1-RMSHE ($r = 2$)).

4.2. Experiments with Color Images

The majority of image enhancement methods found in the literature, including our previous works [12, 13], assesses the contrast improvement of the output image by visually comparing it to the original one. In [12, 13], we claimed that it is difficult to judge a processed enhanced image using a subjective assessment. Hence, in this work, we use two types of quantitative measures to assess the original and processed images produced by the C$1D$HE and TV$3D$HE method and ours (presented in Section 3), and then perform an objective comparison among them.

The first quantitative measure used is a color image quality measure (CIQM) [24], defined by the image color nat-

Method	L^*	L^{RGB}	Q	CNI	CCI
Original	12.53 ± 3.98	31.13 ± 9.90	0.68 ± 0.02	0.81 ± 0.03	0.80 ± 0.12
C1DHE	18.38 ± 3.78	47.11 ± 9.76	0.68 ± 0.01	0.78 ± 0.03	1.03 ± 0.13
HP1DHE	18.14 ± 3.71	46.73 ± 9.61	0.66 ± 0.02	0.78 ± 0.04	0.78 ± 0.07
HP2DHE	18.55 ± 3.91	47.02 ± 10.01	0.67 ± 0.02	0.78 ± 0.04	0.91 ± 0.10
TV3DHE	13.30 ± 2.89	36.44 ± 7.72	0.58 ± 0.02	0.72 ± 0.02	0.49 ± 0.05

Table 2. Contrast for the images in the $CIELUV$ and RGB color spaces and Color Image Quality Measures

uralness and colorfulness indexes, and applied to verify if the HE methods preserve the quality of the images. The second measure refers to the contrast in the $CIELUV$ and in the RGB color spaces, and aims to show how much the HE methods improve the contrast of the original image.

This section presents and discusses the numerical results obtained by using the CIQMs and the contrast measure above mentioned and detailed described in [15, Section 5.1] and [10, Section 5.2.2.1] to evaluate our proposed methods (HP1DHE and HP2DHE) and the others (C1DHE and TV3DHE) in a data set of 300 images taken from the University of Berkeley [8].

We compute, for both the original and the processed images, the contrast in both the $CIELUV$ and RGB color spaces and the CIQMs, as showed in Table 2. Table 2 is divided in three parts. In the first part, we present the image source name, *i.e.*, the original or the methods that originated the image. In the second and third parts, we show the values obtained for the contrast and CIQMs, respectively. Note that the values in the table are presented in the form $\mu \pm \sigma$, *i.e.*, the mean and standard deviation of the measures computed on the data set of 300 images. All images used in this experiment can be seen in [11].

From the second part of Table 2, we observe that the images processed by our methods, *i.e.*, HP1DHE and HP2DHE, have the value of contrast increased, in average, about 50% in both the $CIELUV$ and RGB color spaces. The values of the contrast of images processed by the C1DHE method also increase in a similar fashion. In contrast, the TV3DHE method is the one that increases the less the contrast. Remark that, in general, the improvement of the value of contrast in the $CIELUV$ color space is proportional to the one in the RGB space (the range of the $CIELUV$ luminance is $[0, 100]$ and the RGB luminance is $[0, 255]$ (with $L = 256$)). From this first analysis, we state that our methods and the C1DHE are effective in yielding significant increasing in the value of image contrast.

In the third part of Table 2, we find the Q, CNI, and CCI measures for the original and processed images. Note that the third numerical column in this table reports the Q measure values, which are a weighting function of the CNI and CCI measures. We observe that, in average, the images processed by our methods have preserved values of Q in the processed images close to the value in the original ones. This means that our methods produce images with quality similar to the original images. Also note that the images enhanced by the C1DHE method have obtained similar Q values to the ones obtained by our methods. In contrast, the images produced by the TV3DHE method have Q values quite smaller than the ones calculated from the original images. This shows that the TV3DHE method yields images with deteriorated color quality.

On the fourth numerical column of Table 2, we have the values for the CNI measure. Observe that, in average, our methods and the C1DHE keep the naturalness of the produced images close to the one in the original image, whereas the images produced by the TV3DHE method have CNI values significatively smaller than the ones obtained from the original images.

On the fifth numerical column of Table 2, we report the values for the CCI measure. Observe that the CCI measure is based on the mean and standard deviation of the saturation of the image in the $CIELUV$ color space. The results reported show that, in average, the C1DHE method is the one that more frequently increases the value of the CCI measure from the original to the processed images. The C1DHE method achieves such result because it equalizes the three R, G, and B $1D$ histograms freely and separately. On the other hand, it has the well-known drawback of not being hue-preserving, which will be discussed and illustrated further in this section. The images produced by the TV3DHE method, in average, do not preserve both the CNI and CCI values and, consequently the Q value, close to the values of the original images. The fact that the TV3DHE method produces images with CCI values quite different from the ones in the original images corroborates the hypothesis subjectively stated in [12] and [13] that the TV3DHE method produces overenhanced / undersatured images (*i.e.*, brighter images). That is, in general the saturation values of the images produced by the TV3DHE method are smaller than the saturation values of the images produced by the other methods, and so are their variances.

From the analysis regarding the contrast and the CIQMs, we claim that: 1) The contrast of the images processed by our methods is in average 50% greater than the contrast of

(a) (b) (c) (d) (e)

Figure 2. Results for the landscape image: (a) original image; (b) C$1D$HE; (c) TV$3D$HE; (d) our HP$1D$HE; (e) our HP$2D$HE.

Method	Color Quality			Contrast	
	Q	CNI	CCI	$CIELUV$	RGB
Original	0.7038	0.8540	0.7196	7.00	17.03
C$1D$HE	0.7681	0.9292	0.8089	12.09	30.32
HP$1D$HE	0.7210	0.8725	0.7575	11.50	28.98
HP$2D$HE	0.6504	0.7688	0.8381	11.00	27.59
TV$3D$HE	0.7140	0.9004	0.4392	8.76	23.68

Table 3. Color Image Quality and Contrast Measures for the Images in Figure 2.

the original images, whilst the color quality, measured by the naturalness and colorfulness indexes, of the processed images are close to the ones of the original image; 2) The TV$3D$HE method is the one that show the smaller improvement on the contrast of the original image. Moreover, it produces images overenhanced, deteriorating the color quality of the images; 3) The results achieved for contrast enhancement and color quality preservation by the C$1D$HE method are as good as our methods.

Note that we could perform changes in the TV$3D$HE method in order to make it faster and hue-preserving, by applying our shift hue-preserving transform. Nonetheless, even after these modifications, the images enhanced by the TV$3D$HE method would continue to be overenhanced and the contrast improvement would not be significant.

Despite the good results that our numerical analysis attributed to the C$1D$HE method, and the fact that it is six times faster than our methods, the C$1D$HE is not suitable for real-world applications: the images produced by this method do not preserve the hue of the original image. As a result, the images produced by the C$1D$HE method may have unnatural colors, even though the CNI, CCI, and, consequently, Q, indicate that the images produced by the C$1D$HE method have image color quality close to the ones of the original images. These contradictory results show that the CQIMs used in this work have a drawback. They can quantitatively represent the color quality of a image by means of the naturalness and colorfulness indexes, but they do not take into account simultaneously the original and processed images in such assessment.

In order to exemplify the conclusions reached, we will careful analyze one example of an image extracted from the 300 presented in the data base, named “landscape”. Table 3 shows the contrast and the CNI, CCI, and Q values for the original and processed landscape images in Figure 2. Figure 2(b) shows the landscape image processed by the C$1D$HE method, and highlights the fact that it is not hue-preserving. We observe that the colors present in the image in Figure 2(b) look unnatural with respect to the original image in Figure 2(a), even though the CNI, CCI, and Q values of the processed image are close to the ones in the original image. We can also observe that the image produced by the TV$3D$HE method in Figure 2(c) is overenhanced, *i.e.*, the colors are undersaturated, as explained before in this section. Moreover, we can see that the increase in the value of the image contrast produced by the TV$3D$HE method is the smallest among the compared methods, as shown in Table 3.

Finally, the claims about our methods are verified in the images in Figures 2(d) and 2(e) and confirmed in Table 3. As observed, the images have their contrast value increased by, in average, 50%, while their color quality measures are kept close to the ones of the original image. Besides, our methods are hue-preserving.

5. Conclusions

In the first part of this work, we proposed and tested a new framework called the MHE for image contrast enhancement and brightness preserving which generated natural looking images. The experimental results showed that our methods are better at preserving the brightness of the processed image (in relation to the original one) and yield images with natural appearance, at the cost of contrast enhancement. The contributions of this part of the work are threefold: 1) An objective comparison among all the HE methods using quantitative measures such as the $PSNR$, brightness, and contrast (the comparison of these last two measures can be seen in [14, 10]); 2) An analysis showing the boundaries of the HE technique and its variations (*i.e.*, Bi- and Multi-HE methods), for contrast enhancement, brightness preserving and natural appearance; 3) Our proposed methods.

In the second part of this work, we presented two fast hue-preserving HE methods based on $1D$ and $2D$ histograms of the RGB color space for image contrast enhancement. The HP1DHE and HP2DHE methods have time and space complexities that comply with real-time application requirements. Although the C1DHE method is six times faster than ours, it is not hue preserving. We evaluated the resulting images objectively by using measures of contrast, naturalness and colorfulness [24] on a data set composed of 300 images, such that a quantitative comparison could be performed. The experimental results showed that the value of the contrast of the images produced by our methods is in average 50% greater than the original value. Simultaneously, our methods keep the quality of the image in terms of naturalness and colorfulness close to the quality of the original image. In practice, our methods enhance 512×512 image pixels in 100 milliseconds on a Pentium 4 - 2GHz.

Recall that both proposed methodologies are suitable for real-time and real-world applications.

Acknowledgment

This work was supported by the CNPq/MCT and CAPES-COFECUB/MEC, Brazilian Government's research support agencies and by French Government grant ANR SURF NT05-2_45825 . The first author is very grateful to Prof. Dr Hugues Talbot, for financial providing support during part of his stay in France, where a substantial part of this work was developed.

References

[1] S.-D. Chen and A. Ramli. Contrast enhancement using recursive mean-separate histogram equalization for scalable brightness preservation. *IEEE TCE*, 49(4):1301–1309, Nov. 2003.

[2] S.-D. Chen and A. Ramli. Minimum mean brightness error bi-histogram equalization in contrast enhancement. *IEEE TCE*, 49(4):1310–1319, Nov. 2003.

[3] D. Coltuc, P. Bolon, and J.-M. Chassery. Exact histogram specification. *IEEE TIP*, 15(5):1143–1152, May 2006.

[4] CVG-URG. Image database, 2007. `http://decsai.ugr.es/cvg/dbimagenes/`.

[5] R. Gonzalez and R. Woods. *Digital Image Processing*. Prentice Hall, 3rd edition, Jan. 2008.

[6] Y.-T. Kim. Contrast enhancement using brightness preserving bi-histogram equalization. *IEEE TCE*, 43(1):1–8, Feb. 1997.

[7] M. Luessi, M. Eichmann, G. Schuster, and A. Katsaggelos. New results on efficient optimal multilevel image thresholding. In *IEEE ICIP*, pages 773–776, 2006.

[8] D. Martin, C. Fowlkes, D. Tal, and J. Malik. A database of human segmented natural images and its application to evaluating segmentation algorithms and measuring ecological statistics. In *IEEE ICCV*, volume 2, pages 416–423, July 2001.

[9] D. Menotti. Test image, 2007. `http://wavelet.dcc.ufmg.br/MHE/`.

[10] D. Menotti. *Contrast Enhancement in Digital Imaging using Histogram Equalization*. Phd thesis, UFMG - Universidade Federal de Minas Gerais, DCC - Departamento de Ciência da Computação, Apr. 2008. http://wavelet.dcc.ufmg.br/thesismenotti.pdf.

[11] D. Menotti. Test image, 2008. `http://wavelet.dcc.ufmg.br/FHPHEM/`.

[12] D. Menotti, A. P. Melo, A. A. Araújo, J. Facon, and E. M. Sgarbi. Color image enhancement throught 2D histogram equalization. In *IWSSIP*, pages 235–238, 2006.

[13] D. Menotti, L. Najman, A. A. Araújo, and J. Facon. A fast hue-preserving histogram equalization method for color image enhancement using a bayesian framework. In *IWSSIP*, pages 414–417, 2007.

[14] D. Menotti, L. Najman, J. Facon, and A. A. Araújo. Multi-histogram equalization methods for contrast enhancement and brightness preserving. *IEEE TCS*, 53(3):1186–1194, Aug. 2007.

[15] D. Menotti, L. Najman, J. Facon, and A. A. Araújo. Fast hue-preserving histogram equalization methods for color image contrast enhancement. *omitted*, 2008. submitted in August 2008 - http://wavelet.dcc.ufmg.br/fhphem.pdf.

[16] S. Naik and C. Murthy. Hue-preserving color image enhancement without gamut problem. *IEEE TIP*, 12(12):1591–1598, Dec. 2003.

[17] R. Nickalls. A new approach to solving the cubic: Cardan's solution revealed. *The Mathematical Gazette*, 77:354–359, 1993.

[18] N. Otsu. A threshold selection method from grey-level histograms. *IEEE TSMC*, 9(1):41–47, Jan. 1979.

[19] M. Rabbani and P. Jones. *Digital Image Compression Techniques*. Society of Photo-Optical Instrumentation Engineers (SPIE), Bellingham, WA, USA, 1st edition, 1991.

[20] P. Trahanias and A. Venetsanopoulos. Color image enhancement through 3-d histogram equalization. In *IEEE ICPR*, pages 545–548, 1992.

[21] C. Wang and Z. Ye. Brightness preserving histogram equalization with maximum entropy: A variational perspective. *IEEE TCE*, 51(4):1326–1334, Nov. 2005.

[22] Y. Wang, Q. Chen, and B. Zhang. Image enhancement based on equal area dualistic sub-image histogram equalization method. *IEEE TCE*, 45(1):68–75, Feb. 1999.

[23] J.-C. Yen, F.-J. Chang, and S. Chang. A new criterion for automatic multilevel thresholding. *IEEE TIP*, 4(3):370–378, Mar. 1995.

[24] S. Yendrikhovskij, F. Blommaert, and H. de Ridder. Perceptually optimal color reproduction. In *Proceedings of the Human Vision and Electronic Imaging III*, volume 3299, pages 274–281. SPIE, 1998.